

Hanford Geophysical Logging Project

**Recalibration of a High-Rate Logging System
for Characterization of Intense Radiation Zones
at the Hanford Site**

September 2001

Prepared for
U.S. Department of Energy
Grand Junction Office
Grand Junction, Colorado

Prepared by
MACTEC-ERS
Grand Junction Office
Grand Junction, Colorado

Approved for public release; distribution is unlimited.
Work performed under DOE Contract No. DE-AC13-96GJ87335.

Contents

| | Page |
|--|------|
| Signature Page | iv |
| 1.0 Introduction..... | 1 |
| 2.0 HRLS Calibration Function | 2 |
| 2.1 Calibration Standards | 2 |
| 2.2 Calibration Measurements..... | 3 |
| 2.3 Data Analysis..... | 4 |
| 2.4 Calibration Function..... | 6 |
| 3.0 Tungsten Shield Corrections..... | 10 |
| 4.0 Revised Field Verification Criteria | 15 |
| 5.0 Summary..... | 17 |
| 5.1 Dead Time Correction | 17 |
| 5.2 Tungsten Shield Corrections | 18 |
| 5.3 Calibration Function..... | 19 |
| 5.4 Field Verification Criteria | 21 |
| 6.0 Acknowledgements | 23 |
| 7.0 References..... | 24 |

Tables

| | |
|--|----|
| Table 1. Calibration Standard Source Concentrations..... | 3 |
| 2. Reference Standards for Calibration Source Concentrations | 3 |
| 3. Gamma Rays Used for Calibration | 4 |
| 4. Gamma-Ray Intensities of the Calibration Standards | 5 |
| 5. Full Energy Peak Intensities from the Calibration Spectra..... | 6 |
| 6. Calibration Function Values..... | 6 |
| 7. The New Calibration Function Compared to the Baseline Calibration Function | 9 |
| 8. Calculated Corrections for Each Shield Configuration..... | 12 |
| 9. Tungsten Shield Corrections for the 661.6-keV Gamma Ray..... | 13 |
| 10. Estimated Shield Corrections for the 661.6-keV Gamma Ray..... | 14 |
| 11. Unadjusted Field Verification Acceptance Criteria..... | 15 |
| 12. Field Verification Acceptance Criteria Referenced to April 15, 2001 | 17 |
| 13. Tungsten Shield Corrections for the 661.6-keV Gamma Ray..... | 19 |

Tables (con't.)

| | Page |
|--|-------------|
| Table 14. Calibration Constants for the HRLS Base Calibration and First Recalibration | 21 |
| 15. Field Verification Acceptance Criteria Referenced to April 15, 2001 | 21 |

Figures

| | |
|---|-----------|
| Figure 1. HRLS Calibration Data and Calibration Function | 8 |
| 2. The New Calibration Function Compared to the Base Calibration Function..... | 9 |
| 3. Peak Intensity Data for the 661.6-keV Gamma Ray, Borehole 30-05-07..... | 11 |
| 4. Field Verification Peak Intensities Plotted in Relation to Time | 16 |

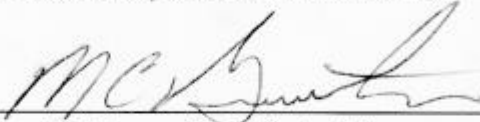
Hanford Geophysical Logging Project

Prepared By:



Carl J. Koizumi, Technical Lead
MACTEC-ERS, Grand Junction Office


09-04-2001
Date



Michael Butherus, Task Order Manager
MACTEC-ERS, Hanford

9/4/01
Date

Concurrence:



James F. Bertsch, Project Manager
MACTEC-ERS, Hanford

9/10/01
Date

1.0 Introduction

During 1995-2000, the U.S. Department of Energy (DOE) Grand Junction Office (DOE-GJO) logged hundreds of existing boreholes around the single-shell tanks (SSTs) at DOE's Hanford Site. Log data were used to develop a baseline characterization of the gamma-ray-emitting radionuclides that are constituents of the radioactive waste that exists in the vadose zone sediments beneath and around the SSTs. These activities were supported by the DOE Richland Operations Office (DOE-RL) and the Office of River Protection (DOE-ORP).

Log data consisted of high-resolution gamma-ray spectra acquired by passive measurements with two types of HPGe detectors. Spectral gamma-ray logging systems (SGLSs) have sondes equipped with 35-percent, p-type, coaxial HPGe detectors (DOE 1995). For cesium-137 (^{137}Cs), which is by far the most widespread radioactive contaminant at Hanford, SGLSs acquired spectra suitable for concentration determinations over a concentration range from a fraction of a picocurie per gram (pCi/g)¹ to about 20,000 pCi/g. When concentrations exceeded about 20,000 pCi/g, the SGLS detectors became "saturated," meaning that the logging systems were unable to record spectra with distinct full energy peaks.

Data for gamma-ray intensities above the SGLS limit were acquired with a high rate logging system (HRLS) that was deployed by DOE-GJO in 1999. The HRLS detector is a low-efficiency planar 6-mm by 8-mm n-type HPGe detector manufactured by EG&G Ortec. The model designation is IGLET-06XXX-S, and the serial number is 39-A314. The crystal is paired with a model 257P resistive feedback preamplifier that was optimized by EG&G Ortec for high count rates. The HRLS acquired useful spectra for ^{137}Cs concentrations up to about 100 million picocuries per gram.

Prior to deployment of the HRLS, measurements were conducted to determine the dead time correction, the calibration function, and energy-dependent corrections for an external tungsten shield that can be installed over the sonde to reduce the gamma-ray flux at the detector and extend the measurement range. Field verification criteria, or tolerances for system operational checks in the field, were also derived. The results are described in a report on the initial, or base, calibration (Koizumi 1999).

To support ongoing SST monitoring measurements and new logging assignments, the HRLS was recalibrated in 2000. In addition, source-specific corrections for a second tungsten shield, alone and in combination with the external shield, were derived. The criteria for field verification system checks were also updated to include data from many additional spectra that have been recorded during field operations with a verification source. The new results are the subject of this report. The corrections for dead time and the external tungsten shield were assumed to be unchanged, and were not investigated for the recalibration.

¹ A picocurie is 10^{-12} of a curie, and a curie is a decay rate of 3.7×10^{10} decays per second.

For the data analysts' convenience, the dead time correction, recalibration results, tungsten shield corrections, and field verification criteria are all presented in Section 5.0, "Summary," of this report.

2.0 HRLS Calibration Function

2.1 Calibration Standards

A calibration center for borehole gamma-ray sensors is located on the Hanford Site near the Meteorology Station, north of the main entrance to the 200 West Area. Heistand et al. (1984) and Steele and George (1986) describe the calibration standards and their links to New-Brunswick-Laboratory-certified standards. These references refer to the eight Hanford calibration standards as the "Spokane SBL/SBH (a pair of standards named SBL and SBH), SBT/SBK, SBU/SBM, and SBA/SBB Models." The "Spokane" designation refers to the original installation of these standards by DOE-GJO in the early 1980s at a calibration facility near Spokane, Washington. The Spokane facility was closed and the standards were moved to DOE's Hanford Site in 1989.

Each standard is a cylindrical block of concrete with a 4.5-inch-diameter test hole coincident with the cylinder axis. The dimensions of the standards (4 feet or 5 feet in diameter, 4 feet thick) are large enough to simulate an "infinite medium," meaning that the gamma-ray flux within the test hole at the center of a standard is equal to the flux that would exist if the medium had the same gamma-ray source concentration, but were infinite in extent.

Each standard has particular concentrations of orthoclase feldspar, uraninite, and monazite. These minerals contain the natural gamma-ray sources. Orthoclase feldspar contains potassium, of which about 0.01 percent is potassium-40 (^{40}K), uraninite contains uranium-238 (^{238}U) and uranium-235 (^{235}U) and the members of the uranium and actinium decay series, and monazite contains thorium-232 (^{232}Th) and the members of the thorium decay series. For the HRLS, the gamma-ray source concentrations of SBT, SBK, SBM, and SBA are too low to produce useful calibration signals. Only SBU, SBL, SBB, and SBH were used, and only the ^{238}U (or radium-226 [^{226}Ra]) concentrations are relevant. The "concentrations" (actually, decay rates per unit mass) of the gamma-ray sources are displayed in Table 1.

Table 1. Calibration Standard Source Concentrations

| Standard | ⁴⁰ K Concentration (pCi/g) | ²²⁶ Ra Concentration ¹ (pCi/g) | ²³² Th Concentration (pCi/g) |
|----------|---|--|---|
| SBU | 10.72 ± 0.84 | 190.52 ± 5.81 | 0.66 ± 0.06 |
| SBL | undetermined | 324 ± 9 | undetermined |
| SBB | undetermined | 902 ± 27 | undetermined |
| SBH | undetermined | 3126 ± 180 | undetermined |

¹ Radium-226 is the fifth decay product of ²³⁸U. If ²²⁶Ra is in decay equilibrium with ²³⁸U, then the concentrations (decay rates per unit mass) of the two nuclides are equal. The ²²⁶Ra concentration is often cited instead of the ²³⁸U concentration because most gamma-ray-based assays utilize gamma rays that originate in nuclides that are below ²²⁶Ra in the uranium decay chain.

Table 2 lists the gamma-ray counting standards to which the source concentrations in the borehole standards are referenced.

Table 2. Reference Standards for Calibration Source Concentrations

| Source | Reference Standard |
|------------------------------|---|
| Potassium (⁴⁰ K) | reagent-grade potassium carbonate (K ₂ CO ₃) |
| Radium (²²⁶ Ra) | NBL (New Brunswick Laboratory) 100-A Series Uranium ¹ |
| Thorium (²³² Th) | NBL 100-A Series Thorium ¹ |

¹ Trahey et al. 1982.

The undetermined concentrations of ⁴⁰K and ²³²Th for SBL, SBB, and SBH impose no limitations on the calibration because the calibration is not source-specific, but relates the intensity of any spectral full energy peak to the source intensity of the corresponding gamma ray, in gamma rays per second per gram of standard material. The spectral full energy peak intensities are calculated from calibration measurements, and the associated gamma-ray source intensities for the calibration standards can be calculated from the known concentrations of ²²⁶Ra in the standards. The actual gamma-ray sources, namely the post-radium nuclides in the uranium series, provide many gamma rays over an ample range of energies for calibration purposes.

2.2 Calibration Measurements

The most common logging parameters at Hanford are:

- Borehole diameter: 6 inches
- Borehole casing: single casing, 0.28-inch-thick steel
- Borehole liquid: none
- Sonde position in borehole: centered (sonde cylindrical axis coincident with borehole axis).

Except for borehole diameter, these nominal borehole conditions were replicated in the calibration measurements so that most log data will not have to be corrected for casing or other borehole environmental effects.

In general, variations in the borehole diameter do not influence the gamma-ray fluxes incident on the sonde if the borehole contains no liquid. Therefore, it is unimportant that the test holes in the calibration standards have smaller diameters (4.5 inches) than the tank farms boreholes (6.0 inches, nominal).

The test holes in the calibration standards are uncased, so a test casing (pipe) made of 0.28-inch-thick steel was installed over the sonde to replicate the casing effect during the calibration measurements.

Calibration data were collected by logging each standard as follows. The logging system was set in the mode for data acquisition with the sonde stationary, the test casing was installed, and the sonde was lowered into the test hole until the center of the detector was at the (vertical) center of the calibration standard. With the sonde held at that position, ten or more spectra were recorded, with a counting time of 1,500 seconds per spectrum.

2.3 Data Analysis

All of the calibration spectra were analyzed with the spectrum analysis program *PCMCA/WIN* (Version 6.3.1, release 13, Aptec Engineering Limited, North Tonawanda, New York). The full energy peak intensities were calculated using the *peaksearch* algorithm in the analysis program. The program algorithm (named *multifit*) that calculates peak areas by Gaussian curve fitting will not be used to analyze field data, and therefore was not used for calibration data analysis. Gaussian curve fitting is inappropriate because the shapes of full energy spectral peaks are often skewed or otherwise affected by pulse pileup and other high rate effects.

Table 3 lists the gamma rays used for the high rate system calibration. Both of the source nuclides (^{214}Pb and ^{214}Bi) are members of the uranium decay series. This recalibration is based on the gamma-ray yields published by Firestone (1999). These yields are only slightly different from the yields published by Erdtmann and Soyka (1979) that were used for the first (base) calibration (Koizumi 1999).

Table 3. Gamma Rays used for Calibration

| Decay Series | Source | Energy (keV) | Yield, Erdtmann and Soyka (gammas per 100 decays) | Yield, Firestone (gammas per 100 decays) |
|------------------|-------------------|--------------|---|--|
| ^{238}U | ^{214}Pb | 241.9 | 7.47 | 7.50 |
| ^{238}U | ^{214}Pb | 295.2 | 19.2 | 18.5 |
| ^{238}U | ^{214}Pb | 352.0 | 37.1 | 35.8 |
| ^{238}U | ^{214}Bi | 609.3 | 46.1 | 44.79 |
| ^{238}U | ^{214}Bi | 1120.3 | 15.0 | 14.8 |
| ^{238}U | ^{214}Bi | 1238.1 | 5.92 | 5.86 |
| ^{238}U | ^{214}Bi | 1764.5 | 15.9 | 15.36 |

The list presented in Table 3 contains no gamma rays with energies less than 241.9 keV, even though gamma rays with energies of 185.7 keV and 186.0 keV are used for SGLS calibrations. These gamma rays have such low intensities that the peaks in HRLS spectra were nonexistent or too small to analyze. The low energy gamma-ray fluxes can be perturbed by the “Z effect” (Koizumi 1999, Koizumi 2000); therefore, the absence of their signals is not necessarily detrimental. In addition, 2204.1-keV and 2614.5-keV gamma rays are used for the SGLS calibrations, but the HRLS detector did not record useful signals for gamma rays with energies higher than 1764.5 keV. The small volume of the HRLS detector allows the higher energy gamma rays to pass through the detector without depositing energy.

Some of the calibration spectra have two prominent peaks, corresponding to energies of about 742.5 keV and 1182.1 keV, which are not observed in SGLS calibration spectra. These are the double escape peaks for the 1764.5-keV gamma ray and the 2204.1-keV gamma ray, respectively. The single escape peaks are not observed. Apparently, if the 1764.5-keV gamma ray, the 2204.1-keV gamma ray, or any other photon undergoes pair production within the detector, both of the positron annihilation photons have a high probability of escaping from the detector because of the detector’s small volume. This point is relevant to analysis of field data because spectra from zones contaminated with ^{60}Co might have a small peak at 310.5 keV corresponding to the double escape peak for the 1332.5-keV ^{60}Co gamma ray.

Table 4 displays the calibration model gamma-ray intensities, in gamma rays per second per gram of material.

Table 4. Gamma-Ray Intensities of the Calibration Standards

| Gamma-Ray Energy (keV) | SBU Gamma-Ray Intensities ($\gamma/\text{s/g}$)¹ | SBL Gamma-Ray Intensities ($\gamma/\text{s/g}$) | SBB Gamma-Ray Intensities ($\gamma/\text{s/g}$) | SBH Gamma-Ray Intensities ($\gamma/\text{s/g}$) |
|-------------------------------|---|---|---|---|
| 241.9 | 0.528 ± 0.016 | 0.899 ± 0.025 | 2.503 ± 0.075 | 8.68 ± 0.50 |
| 295.2 | 1.353 ± 0.041 | 2.221 ± 0.062 | 6.18 ± 0.19 | 21.4 ± 1.2 |
| 352.0 | 2.657 ± 0.080 | 4.37 ± 0.12 | 12.16 ± 0.36 | 42.2 ± 2.4 |
| 609.3 | 3.250 ± 0.099 | 5.38 ± 0.15 | 14.97 ± 0.45 | 51.9 ± 3.0 |
| 1120.3 | 1.060 ± 0.032 | 1.777 ± 0.049 | 4.95 ± 0.15 | 17.14 ± 0.99 |
| 1238.1 | 0.417 ± 0.013 | 0.703 ± 0.020 | 1.958 ± 0.059 | 6.79 ± 0.39 |
| 1764.5 | 1.122 ± 0.034 | 1.842 ± 0.051 | 5.13 ± 0.15 | 17.8 ± 1.0 |

¹Gamma rays per second per gram of material.

Table 5 displays the full energy peak intensities from the calibration spectra. Each peak intensity is the weighted average of the intensities from the group of spectra for the standard designated in the table’s column heading.

Table 5. Full Energy Peak Intensities from the Calibration Spectra

| Gamma-Ray Energy (keV) | SBU Peak Intensities (counts/second) | SBL Peak Intensities (counts/second) | SBB Peak Intensities (counts/second) | SBH Peak Intensities (counts/second) |
|------------------------|--------------------------------------|--------------------------------------|--------------------------------------|--------------------------------------|
| 241.9 | no data | no data | 0.102 ± 0.081 | 0.311 ± 0.061 |
| 295.2 | 0.046 ± 0.012 | 0.074 ± 0.012 | 0.181 ± 0.020 | 0.628 ± 0.039 |
| 352.0 | 0.0557 ± 0.0074 | 0.106 ± 0.011 | 0.292 ± 0.018 | 0.934 ± 0.033 |
| 609.3 | 0.0273 ± 0.0044 | 0.0511 ± 0.0064 | 0.135 ± 0.010 | 0.506 ± 0.020 |
| 1120.3 | no data | no data | 0.0293 ± 0.0092 | 0.074 ± 0.010 |
| 1238.1 | no data | no data | no data | 0.032 ± 0.011 |
| 1764.5 | no data | no data | no data | 0.0082 ± 0.0056 |

2.4 Calibration Function

The calibration function, $I(E)$, is a function of the gamma-ray energy E and is defined as follows:

$$I(E) = \frac{\text{gamma-ray source intensity in gammas per second per gram}}{\text{intensity of the gamma-ray peak in counts per second}}. \quad \text{Eq. (1)}$$

Determining a way to calculate the value of $I(E)$ for any E of interest is the goal of the calibration. After the calibration is accomplished, the measured intensity of any gamma-ray spectral peak can be multiplied by the associated $I(E)$ value to get the gamma-ray source intensity. The gamma-ray source concentration can then be deduced from the source intensity.

Values for the calibration function were calculated for the seven discrete gamma-ray energies using Equation (1) and the source intensities in Table 4 and the peak intensities in Table 5. For each energy, up to four $I(E)$ values were calculated, corresponding to one value for each calibration standard for which a spectral peak intensity was determined. For each energy, a representative value for $I(E)$ was determined by calculating the weighted average of the $I(E)$ values from the various calibration standards. The weighted average values are listed in Table 6.

Table 6. Calibration Function Values

| Gamma-Ray Energy (keV) | $I(E)$ $((\gamma/\text{s/g})/(\text{c/s}))^1$ |
|------------------------|--|
| 241.9 | 27.6 ± 5.4 |
| 295.2 | 33.4 ± 1.7 |
| 352.0 | 44.1 ± 1.3 |
| 609.3 | 104.5 ± 3.5 |
| 1120.3 | 215 ± 26 |
| 1238.2 | 215 ± 77 |
| 1764.5 | 2246 ± 1533 |

¹ Gamma rays per second per gram per count per second.

The gamma-ray energies and calibration function values in Table 6 were analyzed with a curve fitting program to determine a functional relationship that could be used to calculate the values of the calibration function for energies (e.g., 661.6 keV [^{137}Cs]) not represented in the calibration standards. The curve fitting was constrained to use the same function as reported by Koizumi (1999) for the base HRLS calibration:

$$I(E) = \frac{I}{C + D \cdot E \cdot \ln(E) + \frac{F}{E^2}}. \quad \text{Eq. (2)}$$

The factors C , D , and F in Equation (2) are the calibration constants. The values for these constants were established by the curve fitting:

$$\begin{aligned} C &= 0.00568 \pm 0.00090 \\ D &= -4.42 \times 10^{-7} \pm 0.78 \times 10^{-7} \\ F &= 2174 \pm 143. \end{aligned}$$

The units of $I(E)$ will be (gamma rays per second per gram) per (count per second) if E is in kilo-electron-volts.

The uncertainty for $I(E)$ is (Koizumi 1999)

$$\sigma I(E) = (I(E))^2 \cdot \sqrt{(\sigma C)^2 + (E \cdot \ln(E))^2 \cdot (\sigma D)^2 + \left(\frac{1}{E^2}\right)^2 \cdot (\sigma F)^2}. \quad \text{Eq. (3)}$$

The uncertainties σC , σD , and σF in Equation (3) have the values 0.00090, 0.78×10^{-7} , and 143, respectively.

The $I(E)$ values in Table 6 are depicted by small circles in the plot in Figure 1, and the function determined by curve fitting is represented by the smooth curve.

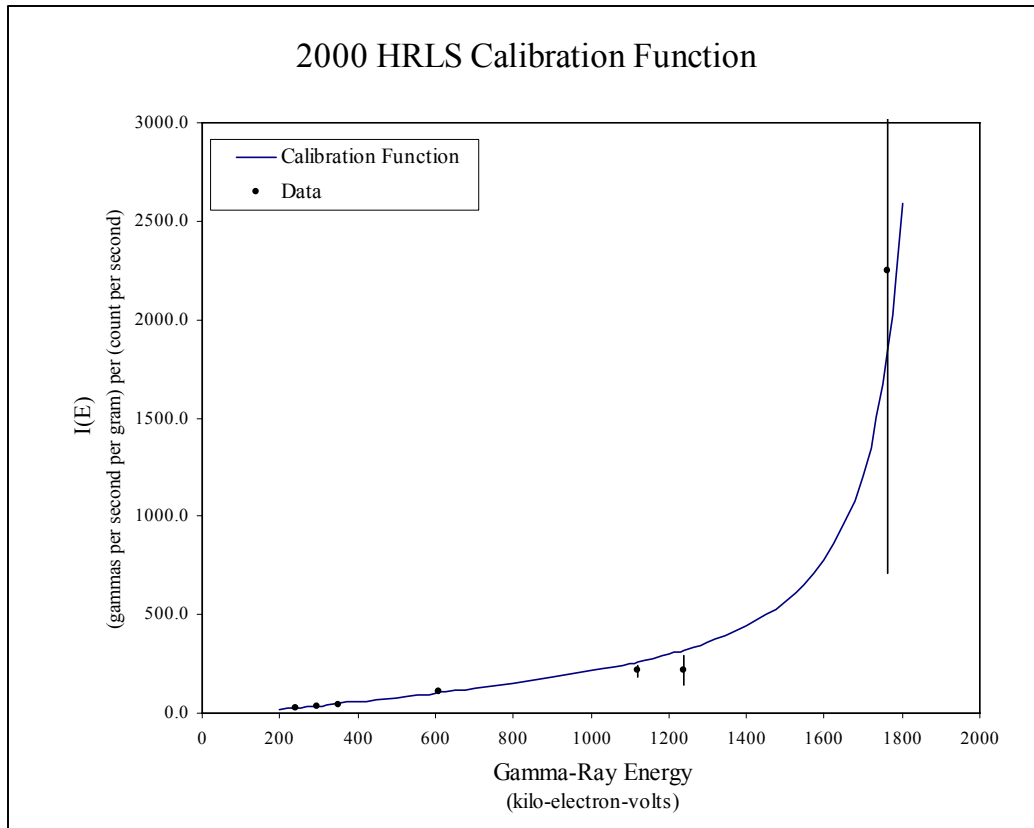


Figure 1. HRLS Calibration Data and Calibration Function. The error bars are not visible on the points representing the lower energies because the lengths of the error bars are smaller than the symbol diameters.

$I(E)$ values calculated with Equation (2) for selected energies are plotted in relation to energy in Figure 2. $I(E)$ values calculated with the base calibration constants are also shown so that the new calibration function can be compared with the previous function.

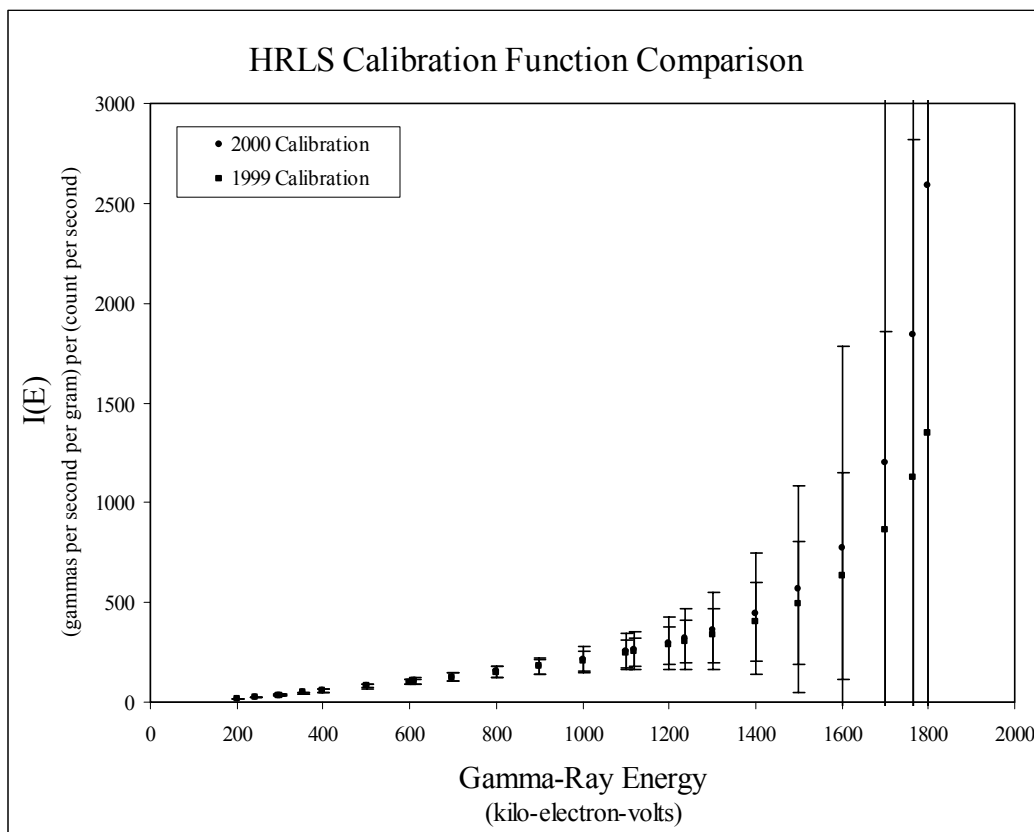


Figure 2. The New Calibration Function Compared to the Base Calibration Function

Table 7 shows calculated $I(E)$ values for some gamma rays of the most common waste constituents. For comparison, values calculated with the base calibration constants are included.

Table 7. Representative $I(E)$ Values Calculated with the Base and New Calibration Functions

| Gamma-Ray Source | Gamma-Ray Energy (keV) | New Calibration Function Value ((γ /s/g)/(c/s)) | Base Calibration Function Value ((γ /s/g)/(c/s)) |
|------------------|------------------------|---|--|
| Cs-137 | 661.6 | 114 ± 13 | 117 ± 17 |
| Co-60 | 1173.2 | 278 ± 86 | 273 ± 87 |
| Co-60 | 1332.5 | 375 ± 165 | 356 ± 152 |
| Eu-152 | 964.0 | 196 ± 40 | 197 ± 45 |
| Eu-152 | 1408.1 | 442 ± 235 | 410 ± 205 |
| Eu-154 | 723.3 | 129 ± 17 | 132 ± 21 |
| Eu-154 | 1274.8 | 335 ± 129 | 322 ± 123 |

The plots in Figure 2 and the entries in Table 7 show that the differences between values predicted by the base and new calibration functions are small (less than 5 percent) for energies less than about 1200 keV. The low energy calibration function values also have smaller uncertainties. These factors suggest that concentrations of radionuclides that emit several gamma

rays should be calculated using the spectral peak for a gamma ray with energy less than 1200 keV, if possible.

3.0 Tungsten Shield Corrections

Two tungsten shields are available to reduce the gamma-ray flux at the HRLS detector during the logging of zones with radiation intensities high enough to saturate the unshielded detector. One shield, named the external shield, is a tungsten pipe that fits over the sonde. The pipe has a 0.31-inch wall thickness. Energy-dependent corrections for the external shield were determined at the base calibration from spectra recorded by logging the SBH standard with and without the shield (Koizumi 1999).

A thicker shield, named the internal shield, is a cup-shaped device that fits over the detector within the sonde housing. The wall thickness of the internal shield is 0.7 inches. This shield is so effective at gamma-ray attenuation that spectra useful for shield correction determinations could not be recorded by logging SBH. Because no calibration standards with radiation intensities higher than those in SBH are available at the Hanford Site, field data had to be used to obtain corrections for the internal shield and the combination of external and internal shields. At this point, data from one Hanford borehole have been used to establish corrections for the 661.6-keV gamma ray of ^{137}Cs .

The data were acquired by logging borehole 30-05-07 in the Hanford “C Tank Farm” (DOE 1998, 2000). After reviewing many SGLS logs, Messrs. R.R. Spatz, A.W. Pearson, and R.G. McCain selected this borehole for the following reasons:

- A large range of ^{137}Cs concentrations permitted acquisition of useful spectra with no shield, and with the internal shield, external shield, and both shields installed.
- The absence of other man-made gamma-ray sources minimized spectrum analysis problems caused by peak interferences and backgrounds with irregular shapes due to Compton continuums from nearby peaks at higher energies.
- A couple of depth intervals had nearly uniform concentrations of ^{137}Cs . This condition was desired mainly because correction data for a particular shield configuration had to be acquired by recording spectra with no shielding, then recording spectra *for the same flux fields* with the shielding installed. This meant that after running a log without shielding, the sonde had to be removed from the borehole, the shielding had to be installed, and the sonde had to acquire the shielded data at depth points as close as possible to the points at which the unshielded data were collected. Because the depth control of the logging system is not perfect, the ability to make multiple measurements in nearly identical flux fields was assisted by the intervals of nearly constant flux.

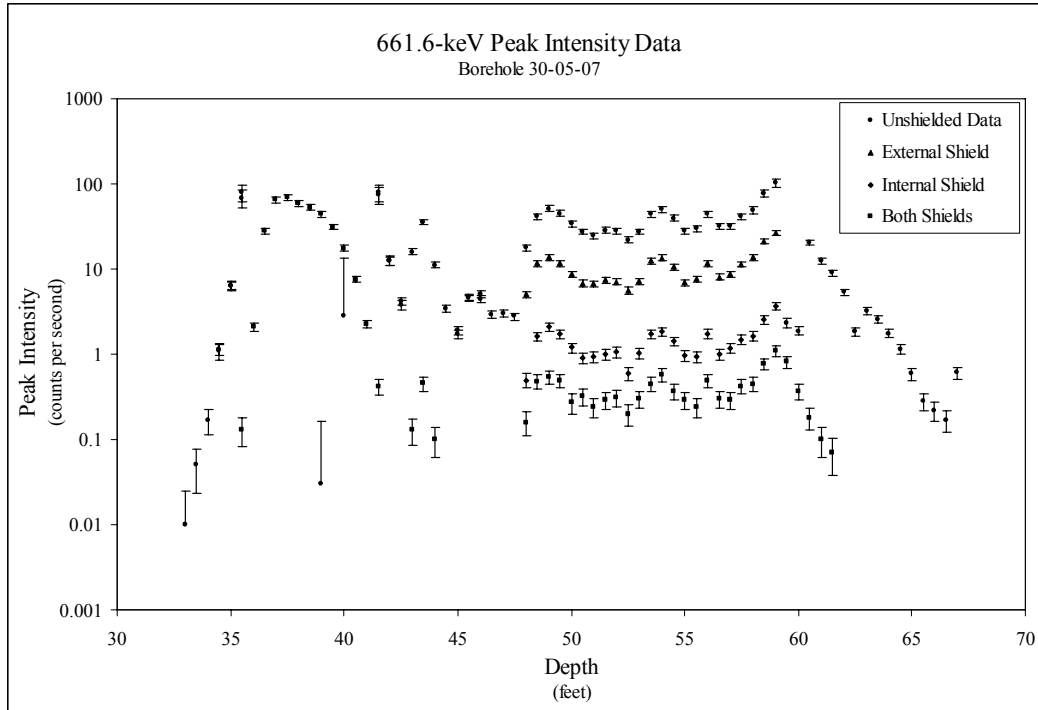


Figure 3. Peak Intensity Data for the 661.6-keV Gamma Ray, Borehole 30-05-07

Figure 3 shows the dead-time-corrected 661.6-keV (^{137}Cs) peak intensity data plotted in relation to depth. These data were used to calculate shield corrections, as follows:

$$\text{correction} = \frac{\text{peak intensity from spectrum recorded without shield}}{\text{peak intensity from spectrum recorded with shield}}. \quad \text{Eq. (4)}$$

Equation (4) indicates that a peak intensity from a spectrum recorded with a shield can be multiplied by the correction to determine the peak intensity that would have been recorded without the shield (if the system were capable of the unshielded measurement). The corrected intensity could then be used for the concentration determination.

For each pair of spectra recorded in the same flux field (i.e., at the same depth), a shield correction value was calculated using Equation (4). The values are displayed in Table 8.

Table 8. Calculated Corrections for Each Shield Configuration

| Depth (feet) | External Shield Correction | Internal Shield Correction | External-Internal Combination Shield Correction |
|-----------------|----------------------------------|----------------------------------|--|
| 35.0 | | | 128.95 ± 72.47 |
| 35.5 | | | 529.34 ± 235.40 |
| 40.0 | | | 0.16 ± 0.59 |
| 41.5 | | | <u>175.33 ± 52.70</u> |
| 43.0 | | | 122.08 ± 42.56 |
| 43.5 | | | 77.33 ± 15.92 |
| 44.0 | | | 110.90 ± 43.48 |
| 44.5 | | | 348.00 ± 523.55 |
| 45.0 | | | 915.79 ± 3821.45 |
| 45.5 | | | 67.43 ± 30.74 |
| 46.0 | | | 63.13 ± 27.06 |
| 46.5 | | | 1536.84 ± 6347.10 |
| 47.0 | | | 302.00 ± 437.49 |
| 47.5 | | | 926.67 ± 2183.50 |
| 48.0 | 3.54 ± 0.41 | 35.56 ± 7.05 | 110.56 ± 35.81 |
| 48.5 | 3.51 ± 0.39 | 25.36 ± 3.56 | 85.54 ± 17.25 |
| 49.0 | 3.76 ± 0.42 | 24.67 ± 3.35 | 94.87 ± 18.77 |
| 49.5 | 3.83 ± 0.42 | 25.97 ± 3.63 | 91.53 ± 18.81 |
| 50.0 | 3.89 ± 0.43 | 28.45 ± 4.29 | 126.15 ± 34.03 |
| 50.5 | 4.04 ± 0.45 | 30.16 ± 4.90 | 85.69 ± 20.16 |
| 51.0 | 3.61 ± 0.40 | 25.97 ± 4.18 | 101.67 ± 27.73 |
| 51.5 | 3.86 ± 0.43 | 29.10 ± 4.66 | 98.79 ± 24.17 |
| 52.0 | 3.95 ± 0.44 | 26.43 ± 4.09 | 89.94 ± 21.13 |
| 52.5 | 3.93 ± 0.45 | 37.10 ± 7.16 | 110.25 ± 32.10 |
| 53.0 | 3.82 ± 0.43 | 26.59 ± 4.14 | 90.83 ± 21.86 |
| 53.5 | 3.57 ± 0.39 | 25.78 ± 3.62 | 97.89 ± 20.58 |
| 54.0 | 3.71 ± 0.41 | 27.47 ± 3.81 | 86.59 ± 16.45 |
| 54.5 | 3.75 ± 0.41 | 27.85 ± 4.07 | 106.43 ± 23.85 |
| 55.0 | 4.01 ± 0.45 | 28.97 ± 4.60 | 96.79 ± 23.73 |
| 55.5 | 3.90 ± 0.43 | 31.80 ± 5.11 | 124.38 ± 33.24 |
| 56.0 | 3.75 ± 0.41 | 25.11 ± 3.48 | 89.51 ± 18.30 |
| 56.5 | 3.95 ± 0.44 | 32.05 ± 5.09 | 105.90 ± 25.65 |
| 57.0 | 3.62 ± 0.40 | 26.93 ± 4.05 | 109.76 ± 27.16 |
| 57.5 | 3.61 ± 0.40 | 27.87 ± 4.03 | 98.21 ± 20.63 |
| 58.0 | 3.60 ± 0.40 | 29.96 ± 4.30 | 109.37 ± 22.78 |
| 58.5 | 3.68 ± 0.45 | 30.46 ± 4.29 | 100.68 ± 18.28 |
| 59.0 | 3.87 ± 0.52 | 27.92 ± 4.07 | 94.61 ± 16.58 |
| 59.5 | | | 2.90 ± 0.58 |
| 60.0 | | | 5.05 ± 1.21 |
| 60.5 | | | 113.06 ± 33.86 |
| 61.0 | | | 123.50 ± 49.18 |
| 61.5 | | | 129.71 ± 59.59 |
| 62.0 | | | 537.00 ± 1210.10 |
| 62.5 | | | 373.47 ± 803.75 |
| 63.0 | | | 321.00 ± 532.53 |
| 63.5 | | | 1523.53 ± 7368.18 |
| 65.0 | | | 210.71 ± 550.59 |

Table 8 has some obvious data outliers. These crossed-out entries were not used in the correction determinations. Data sets with the crossed-out entries removed were analyzed with the Chauvenet criterion (Friedlander et al. 1981), and the double-underlined entry was identified as an outlier that could be rejected. Weighted average corrections for each shield configuration

were calculated, without counting the crossed-out and double-underlined values. Table 9 lists these corrections.

Table 9. Tungsten Shield Corrections for the 661.6-keV Gamma Ray

| Shield | Correction |
|-------------------------------|-------------------|
| external | 3.758 ± 0.088 |
| internal | 27.42 ± 0.89 |
| external-internal combination | 96.4 ± 4.2 |

As mentioned previously, Koizumi (1999) reported an energy-dependent function for calculating the external shield correction. The function is

$$correction = \exp\left(0.43 + \frac{3.31 \times 10^5}{E^2}\right) \quad \text{Eq. (5)}$$

and the uncertainty is

$$uncertainty = correction \cdot \sqrt{(0.15)^2 + \left(\frac{5.4 \times 10^4}{E^2}\right)^2} \quad \text{Eq. (6)}$$

The energy E in Equations (5) and (6) is to be expressed in kilo-electron-volts.

Equations (5) and (6) predict that the external shield correction for $E = 661.6$ keV is 3.27 ± 0.64 .

This agrees, within the uncertainty, with the value 3.758 ± 0.088 derived from the borehole data (Table 9). The value 3.27 ± 0.64 is probably more accurate because it was derived from data that were collected using calibration measurement methods and a calibration standard. In contrast, the value cited in Table 9 was derived from field data that could have been perturbed by variations in the depths of the measurements, nonuniform source distributions, and other uncontrolled factors.

One might expect the correction for the combination of internal and external shields to be equal to the product of the individual corrections for the two shields, but in fact, the product of the external and internal shield corrections (both derived from borehole data), 103.0 ± 4.1 , is slightly greater than the measured correction for the two shields used together (96.4 ± 4.2). This is similar to SGLS casing correction results obtained at the base calibration. For example, the casing data acquired with the SGLS named Gamma 1A indicate that for the 609.3-keV gamma ray, the product of the corrections for 0.33-inch and 0.65-inch casing (total thickness 0.98 inches) is 6.13 ± 0.37 , but the correction derived from 0.98-inch casing measurements is smaller, 5.74 ± 0.24 . Results for various other gamma-ray energies and casing thicknesses indicate that the product of the corrections for two thicknesses T_1 and T_2 is always larger than the correction for the single thickness $T = T_1 + T_2$. Former DOE-GJO contractor employee Dr. R.D. Wilson explained the effect as follows. When the two casings are used separately, the gamma-ray flux

incident on the outer surface of either casing is isotropic. But if one casing is placed inside of the other, the outer casing partially collimates the flux that is incident on the inner casing. The fraction of the flux attenuated by the inner casing is less if the flux is partly collimated instead of isotropic. In effect, the partial collimation of flux makes the correction for the inner casing smaller; therefore, the correction for the two concentric casings is smaller than the correction obtained from the product of the two individual corrections. The discrepancy shrinks as the gamma-ray energy increases because the higher energy gamma rays are not as effectively collimated by the outer casing.

The borehole data for the shielding corrections were acquired over ranges of system dead time, yet the dead-time-corrected peak intensities yielded fairly consistent corrections. This suggests that the dead time corrections are accurate. The accuracy of the dead time correction method has been a matter of concern because some of the spectral peak intensities used to establish the dead time correction function had quite large error bars (Koizumi 1999).

Prior to the determination of shield corrections with field data, Mr. R.G. McCain estimated the corrections using simple attenuation calculations. These calculations simulated a beam of 661.6-keV gamma rays directed at a flat tungsten plate. For a given plate thickness, the correction was defined as the ratio of the incident flux to the (unscattered) flux that emerged on the opposite side of the plate. Table 10 shows the calculated corrections.

Table 10. Estimated Shield Corrections for the 661.6-keV Gamma Ray

| Shield | Correction |
|-------------------------------|------------|
| external | 3.25 |
| internal | 28.1 |
| external-internal combination | 123 |

The values in Table 10 are in reasonable agreement with the corresponding values in Table 9, and, in fact, the external shield correction in Table 10 is closer than the correction in Table 9 to the value (3.27 ± 0.64) predicted by the shield correction equation (Equation [5]). These observations imply that McCain's method can be used to derive good shield correction estimates for other gamma rays, such as the 1173.2-keV and 1332.5-keV gamma rays of ^{60}Co . Some factors that might degrade the accuracy of the method are: (1) the flat plate is not a good representation of the cylindrical shield, (2) in the borehole, the photon flux incident on the outer surface of the shield is nearly isotropic, not collimated in a beam, and (3) the calculations do not account for detector response effects.

The accurate results obtained with McCain's method indicate that the method can also be employed to estimate corrections for thick steel casings. Although no correction is required for the 0.28-inch-thick casing because each calibration measurement was conducted with a section of 0.28-inch-thick casing in the test hole, boreholes at Hanford with different casing thicknesses will surely be encountered in the future. Corrections for casings with thicknesses exceeding 0.28 inches cannot be determined through direct measurements because the test holes of the calibration standards are too small to accommodate such casings along with the sonde.

4.0 Revised Field Verification Criteria

During routine operations, field verification spectra are regularly recorded to check the logging system for proper operation. The field verification gamma-ray source is a custom fabricated sonde collar with a ^{137}Cs button source.

The verification method is based on conventional control chart practice (Taylor 1987). A verification test is conducted by recording a spectrum, then comparing the intensity and full width at half maximum (FWHM) of the 661.6-keV gamma-ray peak to acceptance tolerances. These tolerances are derived from statistical analyses of peak intensities and FWHM from many previously recorded verification spectra. Warning limits are established as the 2-sigma deviations from the mean values of intensity and FWHM, and control limits are established as the 3-sigma deviations:

upper control limit = mean + 3σ

upper warning limit = mean + 2σ

lower warning limit = mean - 2σ

lower control limit = mean - 3σ .

Because 95 percent of readings should fall between the two warning limits, the occurrence of an intensity or FWHM outside of this range suggests the possibility of a logging system malfunction. Essentially all of the readings should fall within the control limits; therefore, the occurrence of a reading outside of the control limits indicates that a logging system malfunction is likely.

Between 08/11/1999 and 08/03/2000, 135 verification spectra were recorded. The means and standard deviations of the peak intensities and FWHM yield the *unadjusted* warning and control limits in Table 11.

Table 11. Unadjusted Field Verification Acceptance Criteria

| Parameter | Warning Limits | | Control Limits | |
|----------------------|----------------|-------|----------------|-------|
| | Lower | Upper | Lower | Upper |
| peak intensity (c/s) | 12.75 | 13.51 | 12.56 | 13.70 |
| FWHM (keV) | 2.10 | 2.59 | 1.98 | 2.71 |

The acceptance criteria in Table 11 are called “unadjusted” because the peak intensities were statistically analyzed without regard to the decay of the source activity in accordance with the somewhat short ^{137}Cs half life of 30.07 years (Firestone and Shirley 1996). Over the one-year period in which verification spectra were recorded, the source output, and hence, the spectral peak intensity, could be expected to decrease by 2.28 percent. A change of this magnitude would presumably be measurable, but changes due to source decay cannot be discerned in the field verification data because all of the spectra but four were collected during a brief four-month period between 08/11/1999 and 12/21/1999.

Small diamond-shaped points in Figure 4 depict the peak intensities plotted in relation to the time of data acquisition. Elapsed time is measured in days, starting at the date of the first spectrum acquisition (08/11/1999). A time gap in the data collection extends from 12/22/1999 to 08/01/2000.

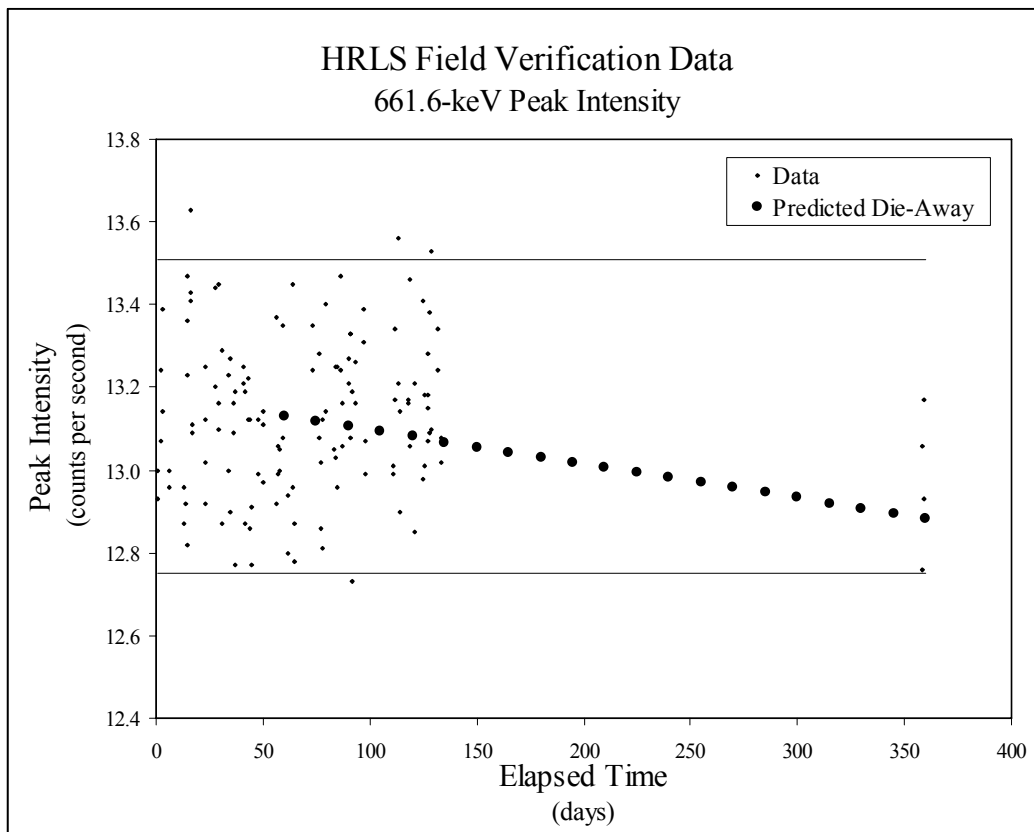


Figure 4. Field Verification Peak Intensities Plotted in Relation to Time

The peaks in the 131 spectra collected in the first four months have a mean intensity of 13.13 counts per second, with a standard deviation of 0.19 counts per second. If 13.13 counts per second is assumed to be the population mean at the midpoint of the four-month period, then the population mean² at later times can be predicted using the radioactive decay equation. The calculations indicate that the decrease in the population mean over time followed the trend depicted by the circular symbols in Figure 4.

The lower and upper warning limits in Table 11 are represented by the horizontal lines in Figure 4. The predicted rate of decline of the mean peak intensity indicates that the mean would reach the lower warning limit just before the end of January 2001. More than half of the peak intensities in verification spectra recorded after that time could be expected to fall below the lower warning limit. This undesirable circumstance can be avoided by adjusting the acceptance criteria in Table 11 to values for a specific date within the period when verification tests will be

² This hypothetical quantity is an estimate of the mean peak intensity that would be determined if a large number of spectra were actually recorded.

performed. The chosen date, April 15, 2001, is close to the midpoint between the 2000 recalibration and the scheduled 2001 recalibration. Table 12 shows the decay-adjusted peak intensity criteria.

Table 12. Field Verification Acceptance Criteria Referenced to April 15, 2001

| Parameter | Warning Limits | | Control Limits | |
|----------------------|----------------|-------|----------------|-------|
| | Lower | Upper | Lower | Upper |
| peak intensity (c/s) | 12.32 | 13.05 | 12.13 | 13.23 |
| FWHM (keV) | 2.10 | 2.59 | 1.98 | 2.71 |

In the future, field verification spectra probably will not be collected within a short time interval, but will probably be more uniformly distributed in time. Each peak intensity should then be decay-adjusted to some point in time, for example, the midpoint between the most recent recalibration and the next recalibration. The acceptance criteria should be derived from the adjusted intensities, and should then be decay-corrected to values appropriate for a date in the middle of the next measurement period.

5.0 Summary

Three new results are described in this report:

- the revised calibration function,
- the corrections for the internal tungsten shield and the combination of external and internal shields, and
- the revised field verification criteria.

Other results, namely the dead time correction and the external tungsten shield correction, are assumed unchanged and have not been revised.

For reference purposes, all of the results, those revised and those unchanged, are presented in this summary.

5.1 Dead Time Correction

The dead time correction reported by Koizumi (1999) was not revised, but is briefly described in this report for the data analysts' convenient reference.

The HRLS dead time effect is negligible for any measurement for which the dead time (T_D) is 10.5 percent or less. When the system dead time exceeds 10.5 percent, a dead time correction can be calculated with

$$K_{DT} = \frac{I}{1.033 - 0.0012 \cdot T_D \cdot \ln(T_D) - 1.6 \times 10^{-6} \cdot (T_D)^3}. \quad \text{Eq. (7)}$$

The dead time correction uncertainty is

$$\sigma K_{DT} = (K_{DT})^2 \cdot \sqrt{(0.069)^2 + (T_D \cdot \ln(T_D))^2 \cdot (0.0014)^2 + (T_D)^6 \cdot (1.9 \times 10^{-6})^2}. \quad \text{Eq. (8)}$$

The correction depends on the dead time but is assumed to be independent of the gamma-ray energy. If the intensity of a spectral peak is P , with uncertainty σP , then the dead-time-corrected intensity is

$$P \cdot K_{DT} \quad \text{Eq. (9)}$$

and the uncertainty in the dead-time-corrected intensity is

$$(P \cdot K_{DT}) \cdot \sqrt{\left(\frac{\sigma P}{P}\right)^2 + \left(\frac{\sigma K_{DT}}{K_{DT}}\right)^2}. \quad \text{Eq. (10)}$$

Because of limitations in the collection of data for the dead time correction determinations (Koizumi 1999), corrections for dead times higher than 56 percent could not be determined. Consequently, the above equations are not valid if the dead time exceeds 56 percent. A dead time of 56 percent corresponds, however, to a very intense gamma-ray flux, so the dead time correction range should be adequate for most, if not all, of the logging at Hanford.

When extreme counting rates are due to high concentrations of uranium or other contaminants with unusually high atomic numbers (Z), the analyst should bear in mind that fluxes of gamma rays with energies less than 500 keV are influenced by the Z effect (Koizumi 1999, 2000). An assay based on a low energy gamma ray will produce a spuriously low concentration. The only remedy is to use the peak for a higher energy gamma ray. No correction for the Z effect has been formulated.

5.2 Tungsten Shield Corrections

When data are recorded with the 0.31-inch-thick external tungsten shield installed, a spectral peak intensity for gamma-ray energy E (expressed in kilo-electron-volts) can be multiplied by the correction calculated with

$$K_{WS} = \exp\left(0.43 + \frac{3.31 \times 10^5}{E^2}\right) \quad \text{Eq. (11)}$$

to compensate for the gamma-ray attenuation by the shield (Koizumi 1999).

The correction uncertainty is

$$\sigma K_{ws} = (K_{ws}) \cdot \sqrt{(0.15)^2 + \left(\frac{5.4 \times 10^4}{E^2} \right)^2} . \quad \text{Eq. (12)}$$

Another shield, known as the internal tungsten shield, is a 0.7-inch-thick tungsten cup that fits over the detector crystal within the sonde. When the external and internal shields are used together, the detector is shielded by more than one inch of tungsten, and the HRLS is able to operate in gamma-ray flux fields corresponding to ^{137}Cs concentrations of 100 million picocuries per gram. The internal shield correction, and the correction for the external-internal shield combination, were derived from borehole data and are applicable to one energy, 661.6 keV (^{137}Cs).

Table 13. Tungsten Shield Corrections for the 661.6-keV Gamma Ray

| Shield | Correction K_{ws} |
|-------------------------------|---------------------|
| internal | 27.42 ± 0.89 |
| external-internal combination | 96.4 ± 4.2 |

If the intensity of a spectral peak is P , with uncertainty σP , then the intensity corrected for shielding is

$$P \cdot K_{ws} . \quad \text{Eq. (13)}$$

The corrected value is the intensity that would have been recorded without the shield, if the system were capable of the measurement.

The uncertainty in the corrected intensity is

$$(P \cdot K_{ws}) \cdot \sqrt{\left(\frac{\sigma P}{P} \right)^2 + \left(\frac{\sigma K_{ws}}{K_{ws}} \right)^2} . \quad \text{Eq. (14)}$$

5.3 Calibration Function

The calibration function,

$$I(E) = \frac{I}{C + D \cdot E \cdot \ln(E) + \frac{F}{E^2}} , \quad \text{Eq. (15)}$$

depends on the gamma-ray energy E explicitly. The values of the calibration constants C , D , and F , were revised on the basis of calibration measurements in 2000. The new values are:

$$\begin{aligned} C &= 0.00568 \\ D &= -4.42 \times 10^{-7} \\ F &= 2174. \end{aligned}$$

These values are appropriate if E is expressed in kilo-electron-volts.

The calibration function uncertainty is

$$\sigma I(E) = (I(E)) \cdot \sqrt{(\sigma C)^2 + (E \cdot \ln(E))^2 \cdot (\sigma D)^2 + \left(\frac{1}{E^2}\right)^2 \cdot (\sigma F)^2} \quad \text{Eq. (16)}$$

and the uncertainties in C , D , and F , are

$$\begin{aligned} \sigma C &= 0.00090 \\ \sigma D &= 0.78 \times 10^{-7} \\ \sigma F &= 143. \end{aligned}$$

Because the calibration function was determined from data recorded with a 0.28-inch-thick test casing installed over the sonde, no casing correction need be applied if the thickness of the casing in the logged borehole is 0.28 inches.

A gamma-ray source intensity, S , is calculated by multiplying the peak intensity P (corrected for dead time and shielding, if necessary) by the value of the calibration function at the gamma-ray energy, E :

$$S = P \cdot I(E). \quad \text{Eq. (17)}$$

The uncertainty in S is

$$\sigma S = S \cdot \sqrt{\left(\frac{\sigma P}{P}\right)^2 + \left(\frac{\sigma I(E)}{I(E)}\right)^2}. \quad \text{Eq. (18)}$$

If $I(E)$ is expressed in (gammas per second per gram) per (count per second), and if P is expressed in counts per second, then the units of S will be gammas per second per gram. The concentration of the gamma-ray source in picocuries per gram is

$$\text{concentration} = \frac{27.027}{Y} \cdot S, \quad \text{Eq. (19)}$$

in which Y is the gamma-ray yield, in gamma rays per decay, and the factor 27.027 is a conversion factor derived from the definition of the curie:

$$1 \text{ curie} = 3.7 \times 10^{10} \text{ decays per second} \Rightarrow 27.027 \text{ pCi} = 1 \text{ decay per second.}$$

Table 14 summarizes the calibration history of the HRLS.

Table 14. Calibration Constants for the HRLS Base Calibration and First Recalibration

| Calibration Constants and Uncertainties | Effective Dates | Reference |
|--|--------------------------------------|----------------|
| $C = 0.0053 \pm 0.0010$ $D = -3.89 \times 10^{-7} \pm 0.67 \times 10^{-7}$ $F = 2.15 \times 10^3 \pm 0.31 \times 10^3$ | 07/02/1999 to 09/13/2000 | Koizumi (1999) |
| $C = 0.00568 \pm 0.00090$ $D = -4.42 \times 10^{-7} \pm 0.78 \times 10^{-7}$ $F = 2174 \pm 143$ | 09/14/2000 to next calibration | This Report |

5.4 Field Verification Criteria

During field operations, the logging engineer regularly checks the operation of the logging system by mounting a ^{137}Cs field verification check source on the sonde, recording a spectrum, and comparing the intensity and FWHM of the peak at 661.6 keV to acceptance tolerances.

The SGLS field verification sources contain radionuclides with long half lives (^{40}K , 1.3×10^9 years; ^{238}U , 4.5×10^9 years; and ^{232}Th , 1.4×10^{10} years), but the ^{137}Cs source in the HRLS verification source has a half life short enough (30.07 years) to warrant adjustments in the peak intensity criteria to account for the decay of the source. Warning and control limits calculated from 131 spectra recorded between 08/11/1999 and 12/21/1999 were adjusted to values appropriate for April 15, 2001.

Table 15. Field Verification Acceptance Criteria Referenced to April 15, 2001

| Parameter | Warning Limits | | Control Limits | |
|----------------------|----------------|-------|----------------|-------|
| | Lower | Upper | Lower | Upper |
| peak intensity (c/s) | 12.32 | 13.05 | 12.13 | 13.23 |
| FWHM (keV) | 2.10 | 2.59 | 1.98 | 2.71 |

A field verification spectrum is assessed as follows. If the peak intensity and FWHM both lie within the corresponding warning limits, the logging system passes the acceptance test, but if both quantities lie outside of the warning limits the acceptance test is failed. If only one parameter value falls outside of the warning limits, another verification spectrum must be recorded and analyzed. If the value of the same parameter falls outside the warning limits (on the same side of the limit range as the first discrepancy) again, the acceptance test is failed. If the parameter value falls outside the warning limits, but on the opposite side of the limit range, then

a third spectrum must be recorded and analyzed, and if the parameter value from the third spectrum also lies outside the warning limits, then the acceptance test is failed.

The logging system fails an acceptance test if a FWHM or peak intensity value falls outside the control limits.

An acceptance test failure should be investigated immediately so that the problem can be corrected as soon as possible.

6.0 Acknowledgments

Ms. R.M. Paxton organized and formatted this material for publication.

Messrs. R.R. Spatz, A.W. Pearson, and R.G. McCain reviewed many SGLS logs and selected the borehole from which the tungsten shield correction data were taken. Mr. A.W. Pearson recorded the correction data, maintaining exquisite depth control during all of the measurements.

Mr. R.G. McCain analyzed the field verification spectra and formulated the warning and control limits for field verification tests.

7.0 References

- Erdtmann, G., and W. Soyka, 1979. *Die Gamma-Linien der Radionuklide (The Gamma Rays of the Radionuclides)*, Verlag Chemie, Weinheim, Germany.
- Firestone, R.B., 1996. *Table of Isotopes* (Eighth Edition), John Wiley and Sons, New York.
- Friedlander, G., J.W. Kennedy, E.S. Macias, J.M. Miller, 1981. *Nuclear and Radiochemistry* (Third Edition), John Wiley and Sons, New York.
- Heistand, B.E., and E.F. Novak, 1984. *Parameter Assignments for Spectral Gamma-Ray Borehole Calibration Models*, GJBX-(284), prepared by Bendix Field Engineering Corporation for the U.S. Department of Energy Grand Junction Projects Office, Grand Junction, Colorado.
- Koizumi, C.J., 1999. *Hanford Tank Farms Vadose Zone Base Calibration of a High Rate Logging System for Characterization of Intense Radiation Zones in the Hanford Tank Farms*, GJO-99-118-TAR GJO-HAN-29, prepared by MACTEC-ERS for the U.S. Department of Energy Grand Junction Office, Grand Junction, Colorado.
- Koizumi, C.J., 2000. *Hanford Tank Farms Vadose Zone Monitoring Project Initial Calibration of the Radiometric Assessment System*, GJO-2001-237-TAR, prepared by MACTEC-ERS for the U.S. Department of Energy Grand Junction Office, Grand Junction, Colorado.
- Steele, W.D., and D.C. George, 1986. *Field Calibration Facilities for Environmental Measurement of Radium, Thorium, and Potassium*, GJ/TMC-01 (Second Edition) UC-70A, prepared by Bendix Field Engineering Corporation for the U.S. Department of Energy Grand Junction Projects Office, Grand Junction, Colorado.
- Taylor, J.K., 1987. *Quality Assurance of Chemical Measurements*, Lewis Publishers, Inc., Chelsea, Michigan.
- Trahey, N.M., A.M. Voeks, and M.D. Soriano, 1982. *Grand Junction/New Brunswick Laboratory Interlaboratory Measurement Program: Part I -- Evaluation; Part II -- Methods Manual*, Report NBL-303, New Brunswick Laboratory, Argonne, Illinois.
- U.S. Department of Energy, 1995. *Vadose Zone Monitoring Project at the Hanford Tank Farms Calibration of Two Spectral Gamma-Ray Logging Systems for Baseline Characterization Measurements in the Hanford Tank Farms* (Rev. 0), GJPO-HAN-1, prepared by Rust Geotech for the U.S. Department of Energy Grand Junction Office, Grand Junction, Colorado.
- U.S. Department of Energy, 1998. *Hanford Tank Farms Vadose Zone C Tank Farm Report*, GJO-98-39-TAR GJO-HAN-18, prepared by MACTEC-ERS for the U.S. Department of Energy Grand Junction Office, Grand Junction, Colorado.

U.S. Department of Energy, 2000. *Hanford Tank Farms Vadose Zone Addendum to the C Tank Farm Report*, GJO-98-39-TARA GJO-HAN-18, prepared by MACTEC-ERS for the U.S. Department of Energy Grand Junction Office, Grand Junction, Colorado.